Cytotoxicity and genome-wide microarray analysis of intestinal smooth muscle cells in response to hexavalent chromium induction

Li-Fang JIN, Yuan-Yuan WANG, Zi-Dong ZHANG, Yi-Meng YUAN, Yi-Rui HU, Yang-Feng WEI, Jian NI*

College of Life Science of Shaoxing University, Shaoxing Zhejiang 312000, *China*

Abstract: Chronic ingestion of high concentrations of hexavalent chromium [Cr(VI)] in drinking water induces intestinal tumors in mice; however, information on its toxicity on intestinal smooth muscle cells is limited. The present study aimed to assess the *in vitro* and *in vivo* toxicological effects of Cr(VI) on intestinal smooth muscle cells. Human intestinal smooth muscle cells (HISM cells) were cultured with different concentrations of Cr(VI) to evaluate effects on cell proliferation ability, oxidative stress levels, and antioxidant system. Furthermore, tissue sections in Cr(VI) exposed rabbits were analyzed to evaluate toxicity on intestinal muscle cells *in vivo*. Gene chips were utilized to assess differential gene expression profiles at the genome-wide level in 1 μmol/L Cr(VI) treated cells. Intestinal tissue biopsy results showed that Cr(VI) increased the incidences of diffuse epithelial hyperplasia in intestinal jejunum but caused no obvious damage to the structure of the muscularis. Cell proliferation analysis revealed that high concentrations (≥64 μmol/L) but not low concentrations of Cr(VI) (≤16 μmol/L) significantly inhibited the growth of HISM cells. For oxidative stress levels, the expression of reactive oxygen species (ROS) and nitric oxide (NO) was elevated at high concentrations (≥64 μmol/L) but not at low concentrations of Cr(VI) (≤16 μmol/L). In addition, dose-dependent increases in the activity of oxidized glutathione (GSSH)/total-glutathione (T-GSH) were also observed. Gene chip screened 491 differentially expressed genes including genes associated with cell apoptosis, oxidations, and cytoskeletons. Some of these differentially expressed genes may be unique to smooth muscle cells in response to Cr(VI) induction.

Keywords: Intestinal smooth muscle cells; Hexavalent chromium; Cytotoxicity; Gene chip

Heavy metals toxin exposure can impact human and animal health (Liu et al, 1991; Smith, 2008). Hexavalent chromium [Cr(VI)] is considered carcinogenic to humans (Group 1) by the International Agency for Research on Cancer (IARC) and evidence on lung carcinogenic effects of Cr(VI) has been fully described in previous reports (Park & Stayner, 2006; Smith, 2008). In addition, epidemiologic studies have indicated that exposure to Cr(VI) may damage the liver (Rafael et al, 2007; Yuan et al, 2012), kidneys (Velma & Tchounwou, 2011), reproductive system (Subramanian et al, 2006), and immune system (Raghunathan et al, 2009). Hexavalent chromium can be inhaled or administered intratracheally, intraperitoneally, intravenously, or orally. Oral ingestion of contaminated foods and drinking well-water is the main source of non-occupational exposure to Cr(VI). Previous research has shown that human population exposure to Cr(VI) in drinking water resulted in a statistically significant increase in stomach tumors (Zhang & Li, 1997). More recently, administration to rodents of Cr(VI) in drinking water resulted in statistically significant increases in papillomas and carcinomas (combined) of the oral cavity and small intestine in high dose groups (Stout et al, 2009). To further elucidate key events underlying toxicity of Cr(VI) on the intestine, Kopec et al (2012) analyzed differential gene expression patterns in intestinal samples following 7 or 90 days exposure to different concentrations of Cr(VI) in drinking water, and showed expression levels of genes related to oxidative stress, cell cycle, lipid metabolism, and immune response changed in a dose-dependent way with Cr(VI) exposure. These results strongly suggest that Cr(VI) escaping from stomach reduction could be toxic to the gastrointestinal tract by

Received: 26 November 2012; Accepted: 10 January 2013
Foundation items: Zhejiang Natural Sciences Foundation Y2110911
* Corresponding author, E-mail: nijian@usx.edu.cn

changing the expression level of genes.

Intestinal smooth muscle cells provide structural support for many tissues and control essential physiological processes such as gastrointestinal motility and blood pressure. In digestive systems, rings of smooth muscle, called sphincters, regulate movement of materials along internal passageways and push contents through the central lumen. Studies have suggested that Cr(VI) has an adverse effect on intestinal epithelial tissue/cells; so far, however, available information on toxicity effects of Cr(VI) on intestinal smooth muscle cell is limited. Because Cr(VI) as chromate structurally resembles sulfate and phosphate, it can be taken up by all cells and organs throughout the body through nonspecific anion transporters. In addition, the expression of genes in a given cell is very different compared to those expressed in the other cells. Therefore, Cr(VI) may induce unique gene expression patterns for a given cell. Microarray analysis can provide quantitative gene expression information at the genome-wide level and help discover novel changes in genes expression, which may be unique to given cells. Therefore, the purpose of our study was to evaluate the effect of Cr(VI) on the cytotoxicity of intestine smooth muscle cells, and screen differentially expressed genes to identify novel changes in gene expression profiles by gene chip in intestinal smooth muscle cells in response to Cr(VI) induction.

MATERIALS AND METHODS

Animal model design

Groups of 12 male and 12 female New Zealand white rabbits were exposed to potassium dichromate ($K_2Cr_2O_7$) in drinking water at concentrations of 0, 7, or 41.8 mg/L Cr(VI) for 3 months (equivalent to average daily doses of approximately 0, 0.35, and 2.09 mg Cr(VI)/kg body weight per day per rabbit). Animals were observed twice daily and clinical findings were recorded. After exposure to Cr(VI) for 3 months, jejuna of the intestines were fixed and preserved in 10% neutral buffered formalin, trimmed and processed, embedded in paraffin, sectioned to a thickness of 4–6 μm, and stained with hematoxylin and eosin (H&E) for microscopic examination (Nikon, Japan). The Institutional Animal Care and Use Committee(s) (IACUC) at the College of Life Science of Shaoxing University approved all procedures performed on the animals (approval number: S20110018).

Cell Culture

Human intestinal small muscle cells (HISM cells) from the American Type Culture Collection (ATCC) were cultured in DMEM (Invitrogen, CA) supplemented with 10% FBS (Hyclone, UT), 100 U/mL penicillin (Invitrogen, CA), and 100 mg/ml streptomycin (Invitrogen, CA). Cells were cultured at 37 °C in an incubator with a humidified atmosphere containing 5% CO_2. Media were changed every other day, and cells were split every 4 days. For Cr (VI) exposure, cells were exposed to 0, 0.25, 1, 4, 16, 64, and 128 μmol/L Cr(VI).

3-(4,5-cimethylthiazol-2yl)-2,5-diphenyl tetrazolium bromide (MTT) assay

Cells at the growth log phase for each group were inoculated into 96-well plates at 100 μL/well. Ten microliters of MTT (5 mg/mL) was added to each well before termination. Plates were incubated at 37 °C in 5% CO_2 for 4 h. The supernatant was discarded and DMSO (100 μL/well) was added. The mixtures were shaken gently to dissolve the hyacinth in sediment. Absorbance (A) values at a wavelength of 492 nm were detected by a microplate reader (Authos, Austria), and the cell proliferation rate was then calculated.

Cell growth curve assay

Briefly, 1×10^4/L cells in the logarithmic growth phase were harvested and seeded on 12-well plates overnight. Different concentration (0, 0.25, 1, 4, 16, 64, and 128 μmol/L) of Cr(VI) was administrated into the culture medium, and the cells were further incubated for 4 days. After incubation, cell viability was determined by trypan blue dye exclusion. A growth curve was drawn according to the logarithmic number of cells/L with incubation time. Multiplication time and growth saturation density were calculated based on the curve.

Measurement of nitric oxide (NO) production

After culturing with different concentrations (0, 0.25, 1, 4, 16, 64, and 128 μmol/L) of Cr(VI) for 30 min, total NO production was estimated by spectrophotometric measurement of nitrite and nitrate concentrations in the cell culture supernatant fluid using Griess reagent with the Total Nitric Oxide Assay Kit (Beyotime Ins. Bio, China) according to manufacturer's instructions. Optical density at 540 nm was measured by a microplate reader (Authos, Austria). Concentrations were calculated by comparing absorptions with those of the standard curve.

Determination of cellular reactive oxygen species (ROS)

To determine intracellular accumulation of ROS in HISM cells, the membrane permeable indicator dihydrodichlorofluorescein diacetate (H2DCF-DA) (Nanjing Jiancheng Corp, China) was employed. The HISM cells treated with Cr(VI) for 24 h were loaded with 10 μmol/L H2DCF-DA in serum-free medium at 37 °C for 90 min, and then washed twice with PBS and digested by trypsin. Cells were monitored with an inverted fluorescence microscope (Nikon, Japan) at an

excitation wavelength of 488 nm and an emission wavelength of 525 nm. Reactive oxygen species were determined by comparing changes in fluorescence intensity with those of the standard curve.

Oxidized glutathione (GSSH)/total-glutathione (T-GSH) assay

The HISM cells treated with Cr(VI) for 24 h were lysed using liquid nitrogen and GSSH/T-GSH activity was evaluated in cells using the glutathione peroxidase assay kit (Nanjing Jiancheng Corp, China), according to manufacturer's instructions. This assay is based on the oxidation of NADPH to NAD+, catalyzed by a limiting concentration of glutathione reductase, with maximum absorbance at 340 nm by the microplate reader (Authos, Austria).

Microarray hybridization and data analysis

Microarray analysis was conducted using Agilent Human Whole Genome 8×60 k Arrays to analyze ~40 000 transcripts. Total RNA from 1 μmol/L Cr(VI) treated or untreated samples was isolated with Trizol reagent (Invitrogen) and then stored at −80 °C. Fifty nanograms of total RNA was converted into labeled cRNA with nucleotides coupled to fluorescent (Cy3) dye using the Quick Amp Kit (Agilent Technologies, Palo Alto, CA) following the manufacturer's protocols. The A260/280 nm ratio and yield of each of the cRNAs were determined and quality assessment was done using an Agilent Bioanalyzer. Equal amounts of Cy3-labeled cRNA from two different samples were hybridized to Agilent Human Whole Genome 8×60 k Microarrays. The hybridized array was washed and scanned and data were extracted from the scanned image using Feature Extraction version 10.2 (Agilent Technologies). Microarray data were normalized using a semi-parametric approach. Unless stated otherwise, gene expression data were ranked and prioritized using fold change>2 criteria to identify differentially expressed genes. Annotation and functional categorization of differentially regulated genes were performed using the Database for Annotation, Visualization and Integrated Discovery (DAVID) and Ingenuity Pathway Analysis (IPA, Ingenuity Systems, Red wood City, CA).

Quantitative reverse transcription polymerase chain reaction (qRT-PCR)

Samples of total RNA were isolated from cells used in microarray hybridization using SYBR Green-based qRT-PCR. Briefly, 0.5 μg of RNA was primed by Oligo$(dT)_{16}$ (Promega, USA) and reverse transcribed using AMV reverse transcriptase in a 20 μL reaction system. From a 2-fold dilution of this cDNA solution, 0.5 μL was used in a 20 μL PCR reaction containing 10 μL SYBR premix Ex Taq, 0.4 μL Rox (TaKaRa, Japan), and 10 μmol/L forward and reverse primers. All primers were designed by submitting RefSeq sequences to Primer Premier 5.0 software; amplicons were approximately 100–200 bp. Primer sequence for MPRIP is 5′-GCTTGGAGGTGCCATATAC-3′/5′-GACCGTTCACTG GATGAAA-3′; for ACTR3B is 5′-CCGCTGTATAA GCCCGAGTT-3′/5′-CAACGTGACACCATCGAACG-3′; for ACTIN is 5′-AGCCTCGCCTTTGCCGATCC-3′/5′-ACATGCCGGAGCCGTTGTCG-3′. The PCR amplifications were conducted in 96-well BIOplastics (Axygen, USA) on an Applied Biosystems PRISM 7300 Sequence Detection System under the following conditions: 10 seconds denaturation and enzyme activation at 95 °C, followed by 40 cycles of denaturation (95 °C, 10 seconds), and annealing (60 °C, 30 seconds). Results were normalized to beta-actin to control for differences in RNA loading, quality, and cDNA synthesis. Amplicon size and reaction specificity were confirmed by agarose gel electrophoresis. Each sample was assayed in triplicate and median threshold cycle values were used to calculate the fold change between treated and control samples.

Statistical Analysis

All data were expressed as means±*SEM*. Statistical comparisons were performed using Student's *t*-test, $P<0.05$ was considered statistically significant.

RESULTS AND DISCUSSION

Intestinal tissue biopsy

The aim of this study was to assess the toxicity of Cr(VI) on intestinal tissue. Intestine sections from rabbits, which ingested Cr(VI)-containing water for 3 months, were proceeded and observed. Consistent with previous studies (Bucher, 2007; Thompson et al, 2011), our results showed a clear exposure concentration response for increased incidences of diffuse epithelial hyperplasia in intestinal jejuna (Figure 1A, 1B, 1C). In the control group, intestinal mucosa was lined with a continuous layer of polarized epithelial cells (Figure 1A1). In contrast, exposure to Cr(VI) resulted in disruption of intestinal epithelial tissue integrity and disorder of the linear arrangement of epithelial cells (Figure 1B1, C1). In contrast to the controls (Figure 3A), the jejuna of the Cr(VI) exposed rabbits had short, broad, blunt epithelial cell layers and generalized mucosal hypercellularity that was particularly prominent in the mucosa crypt (Figure 1A2, B2, C3). Muscularis of the small intestine consists of smooth muscle fibers, and we did not find obvious changes in morphology, muscle fibers and cell nuclei in Cr(VI) induced muscularis tissue compared with those in the untreated group (Figure 1A3, B3, C3).

For the first time, this study provided additional evidence that Cr(VI) was responsible for intestinal

hyperplasia in the rabbit model. However, obvious changes were not found in the morphology, muscle fibers, and cell nuclei of the muscularis in response to Cr(VI) induction, which may be partially explained as: (1) most Cr(VI) escaping from stomach reduction were absorbed by intestinal epithelial cells before penetrating into the muscularis, which resulted in low concentration of Cr(VI) in smooth muscle cells; (2) compared to intestine epithelial cells, smooth muscle cells were not sensitive to toxicity or carcinogenicity of Cr(VI); and or (3) toxicity of Cr(VI) on intestine muscularis was not well reflected at the tissue level.

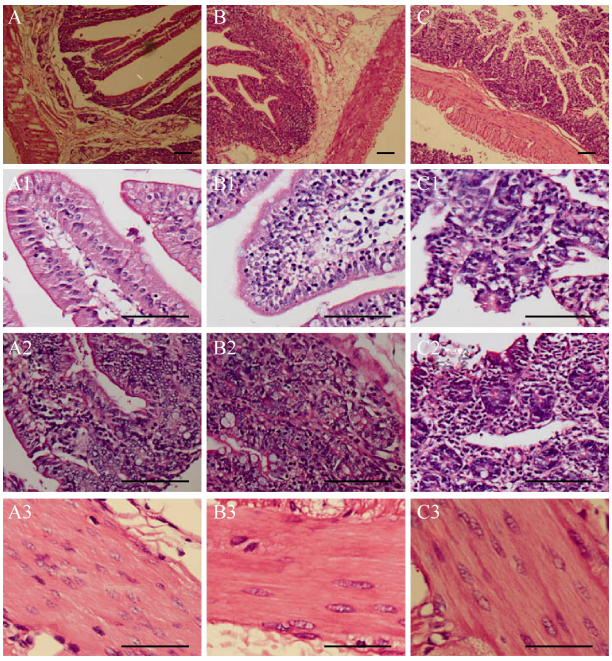

Figure 1 *in vivo* analysis on toxicity of Cr(VI) (0 mg/L (A, A1, A2, A3), 7 mg/L (B, B1, B2, B3) and 41.8 mg/L (C, C1, C2, C3)) on adult rabbit intestines

Low magnification micrograph of small intestine showed diffuse epithelial hyperplasia in jejunum of the 7 mg/L (B) and 41.8 mg/L (C) Cr(VI) treated groups compared to untreated group (A). In contrast to the controls (A1), exposure to Cr(VI) (B1, and C1) resulted in disruption of epithelial arrangement of mucosa. High magnification micrograph of small intestine mucosa showed a short, broad, blunt epithelial cell layer and generalized mucosal hypercellularity in the mucosa crypt in the 7 mg/L (B2) and 41.8 mg/L (C2) Cr(VI) treated groups compared to untreated group (A2). No changes were observed in morphology, muscle fibers and cell nuclei of smooth muscle cells, and thickness of muscularis in Cr(VI) treated or untreated groups (A3, B3 and C3). All sections were stained with hematoxylin and eosin. Bar=200 μm.

Effect of Cr(VI) on cell viability and proliferation

To further study the potential toxic effect of Cr(VI) on smooth muscle cells, we tested the effect of Cr(VI) on the morphology and proliferation of human intestinal small muscle cells (HISM cells) at the cellular level. After treatment with different concentrations (0, 0.25, 1, 4, 16, 64, and 128 μmol/L) of Cr(VI) for 24 hours, the morphology of HISM cells was observed under an inverted phase contrast microscope. At low concentrations of Cr(VI) (≤16 μmol/L), cells maintained a long spindle-shaped fibrocyte-like morphology. However, cells shrunk and became round at high concentrations of Cr(VI) (≥64 μmol/L) (Figure 2A). The MTT assay further revealed that low concentrations of Cr(VI) (≤16 μmol/L) had no effect on cell proliferation, but high concentrations of Cr(VI) (≥64 μmol/L) significantly weakened cell proliferation ability (Figure 2B). Consistent with the MTT assay results, the cell growth curve also showed that high concentrations of Cr(VI) (≥16 μmol/L) decreased the number of HISM cells in a time-dependent manner (Figure 2C). Taken together, consistent with previous studies (Ye & Shi, 2001; Kimura et al, 2011), our results suggest that moderate to high concentrations of Cr(VI) were toxic to HISM cell proliferation.

Detection of ROS and NO

Both ROS and NO play important roles in many cellular signaling pathways, such as proliferation, cell activation, and migration. They can be detrimental when produced in high amounts in intracellular compartments, which is also referred to as “oxidative and nitrosative stress” (Myers et al, 2011). Therefore, experiments were designed to detect the expression levels of ROS and NO in cells with short-term Cr(VI) induction. We found that high concentrations of Cr(VI) (≥64 μmol/L) significantly increased the production of ROS and NO (Figure 3A). In contrast, low concentrations of Cr(VI) (≤16 μmol/L) failed to increase ROS and NO production in HISM cells (Figure 3B). Thus, these results revealed that exposure to high concentrations of Cr(VI) (≥64 μmol/L) resulted in an excessive increase in ROS and NO generation in HISM cells, which could induce cell death as confirmed by cell proliferation analysis.

Assay of GSSH/T-GSH

Cells have an elaborate defense system, such as GSSH/T-GSH, against injurious oxidizing agents. This system helps to maintain steady state concentrations of active oxygen at acceptable levels under physiological conditions. In contrast, inhibition of this defense system can induce a prooxidant state (Myers et al, 2011; Shi & Jiang, 2002). In the present study, the expression levels of GSSH/T-GSH were detected to evaluate the activity of antioxidant systems in Cr(VI) induced cells. After treatment with different concentrations of Cr(VI) for 24 h, activity of GSSH/T-GSH (Figure 3C) increased in a dosage-dependent manner. Increased expression of GSSH/T-GSH indicated that cellular antioxidant systems were activated in response to Cr(VI) to remove extra O^-_2 and H_2O_2.

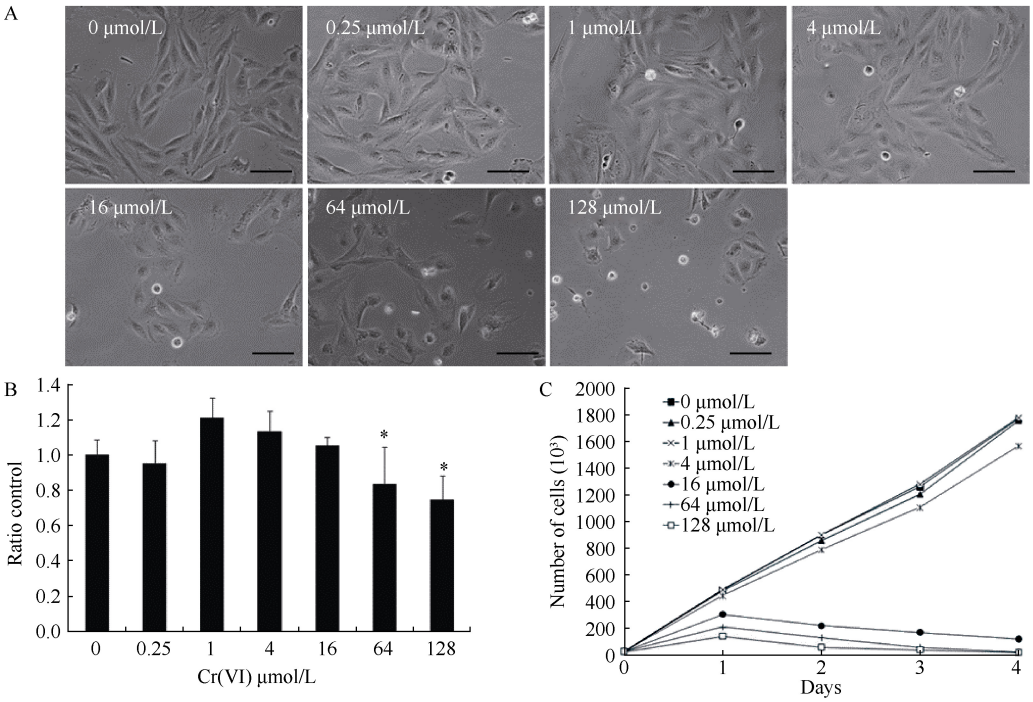

Figure 2 Effect of Cr(VI) on cell morphology and cell number

A: Phase contrast images of HISM cells treated with or without different concentration of Cr(VI); MTT (B) and growth curves (C) assay revealed that high concentration of Cr(VI), but not low concentration of Cr(VI), inhibited growth rate of HISM cells. Data are expressed as means±*SEM* of three independent experiments, *:P<0.05, compare to control group. Bar=100 μm.

Functional annotation and pathway analysis of differentially expressed genes

To investigate gene expression information at the genome-wide level, we analyzed gene expression profiles in HISM cells after exposure to 1 μmol/L Cr(VI) using Agilent human whole genome Microarray Kit. In comparison to control cells, 196 genes were significantly upregulated and 295 genes were significantly downregulated (fold >2). To assess the biological relevance of the differentially expressed genes, we loaded the gene expression data into GeneSpring to sort differentially expressed genes into determined gene ontology groups. Gene ontology (GO) terms and Kyoto Encyclopedia of Genes and Genomes (KEGG) pathways with significant over-representation are listed in Table 1.

The 491 differentially expressed genes were then classified into different functional categories according to the GO project for biological process. The main GO categories for differentially expressed genes were related to cell differentiation, protein homoligomerization, positive regulation of protein phosphorylation, mitochondrion organization, sensory perception of taste, endoplasmic reticulum to Golgi vesicle-mediated transport, smooth muscle contraction, and carbohydrate transport. The KEGG pathway analysis component was used to find co-expressed clusters sharing the same pathway. Six signaling pathways were found to be involved in protein processing in endoplasmic reticulum and leukocyte transendothelial migration (Table 1). Therefore, we provided a global view of differential gene expression in HISM cells in response to Cr(VI) induction.

Changes in genes associated with cell apoptosis, actin cytoskeleton, and oxidation

We identified specific genes of interest within the cluster groups. Genes associated with apoptosis, oxidations, and cytoskeletons, and their differential expression patterns are shown in Table 2. Most proapoptosis related genes were downregulated; for example, KLF6 was downregulated 5.66 times, CASP10 was downregulated 4.41 times, and NLRP1 was downregulated 4.25 times. Decreased expression level of apoptosis related genes partially explained the survival and proliferation of HISM cells after exposure to low concentrations of Cr(VI). As previously described (Ye & Shi, 2001, Sun et al, 2011), changes in genes related to oxidative stress in our Cr(VI) exposed cells were also observed, such as NOX4 and MSRB2. Induction of genes associated with oxidative stress explains why there were changes in oxidation and antioxidant systems in HISM cells in response to Cr(VI).

It is worth noting that genes related to smooth muscle contraction changed, including the downregulation of MPRIP (5.20 times) and the upregulation of TTN and

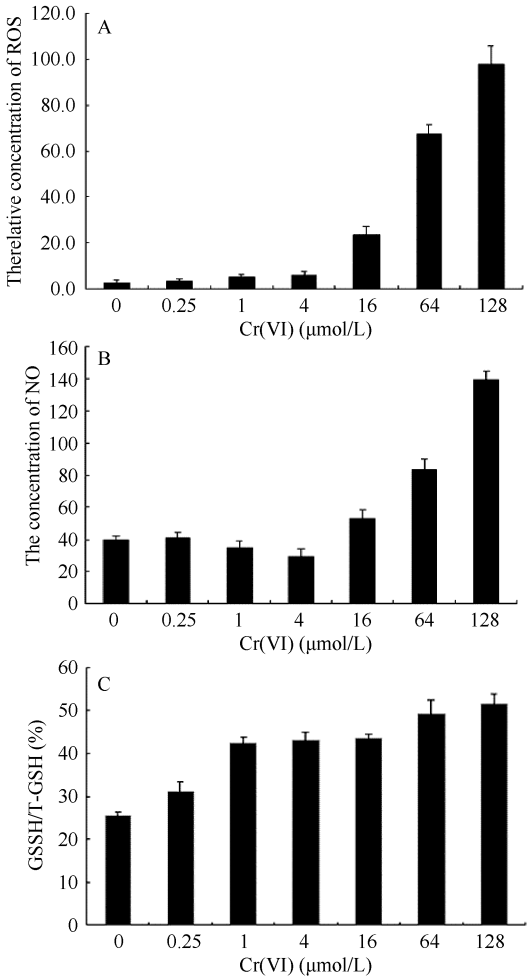

Figure 3 Detection expression level of ROS, NO and GSSH/T-GSH with different concentrations of Cr(VI).

Detection expression levels of ROS, NO and GSSH/T-GSH with different concentrations of Cr(VI). Cr(VI) treatment, especially high dose of Cr(VI) (≥64 μmol/L), increased ROS (A) and NO (B) expression level in HISM cells. Activity of GSSH/T-GSH (C) was unregulated in a dosage-dependent manner. Data were expressed as means±*SEM* of three independent experiments.

MYL7 (2.97 and 2.89 times, respectively). The MPRIP gene targets myosin phosphatase to the actin cytoskeleton through the regulation of actin cytoskeleton by RhoA and ROCK 1. Depletion of MPRIP leads to an increased number of stress fibers in smooth muscle cells through stabilization of actin fibers by phosphorylated myosin. In addition, overexpression of MPRIP as well as its F-actin-binding region leads to disassembly of stress fibbers in neuronal cells (Koga & Ikebe, 2005; Surks et al, 2005). Our data suggested that Cr(VI) may have a potential role in the contraction of smooth muscle cells.

Real time PCR validation of gene expression

To validate our microarray study results, qRT-PCR was performed on a subset of two genes exhibiting a

Table 1 Functional annotation and pathway analysis of genes more than 2-fold in 1 μmol/L Cr(VI) treated cells

Category	GO Term	List hits	*P*-value
GO Biological Process	Cell differentiation	14	0.0438
	Protein homooligomerization	4	0.0402
	Positive regulation of protein phosphorylation	4	0.0199
	Mitochondrion organization	4	0.0012
	Sensory perception of taste	4	0.00311
	ER to Golgi vesicle-mediated transport	3	0.0384
	Smooth muscle contraction	3	0.000948
	Carbohydrate transport	3	0.0167
	COPII vesicle coating	2	0.00955
	Calcium-independent cell-cell adhesion	2	0.0487
	Cardiac muscle fiber development	2	0.00411
	Chondroitin sulfate biosynthetic process	2	0.00751
GO Cellular Component	Integral to membrane	88	0.0167
	Intracellular	44	0.0281
	Membrane fraction	14	0.0373
	Ribosome	9	0.0013
	Transport vesicle	3	0.0284
	Nicotinic acetylcholine-gated receptor-channel complex	2	0.0332
	ER to Golgi transport vesicle membrane	2	0.0262
	COPI coated vesicle membrane	1	0.0337
	SSL2-core TFIIH complex	1	0.017
	Telomeric heterochromatin	1	0.017
	NALP1 inflammasome complex	1	0.017
	Nuclear telomeric heterochromatin	1	0.0337
GO Molecular Function	Ion channel activity	7	0.0121
	Endonuclease activity	4	0.0216
	Extracellular ligand-gated ion channel activity	3	0.0405
	Folic acid binding	2	0.0249
	Nicotinic acetylcholine-activated cation-selective channel activity	2	0.0282
	Acetylcholine receptor activity	2	0.0189
	Acetylcholine binding	2	0.0136
	Carboxylic acid binding	2	0.00393
	Glycolipid binding	2	0.00544
	Taste receptor activity	2	0.0249
	Ribonuclease activity	2	0.0316
	Neuromedin U receptor activity	1	0.0329
KEGG Annotations	Protein processing in endoplasmic reticulum	6	0.0325
	Leukocyte transendothelial migration	5	0.0261
	Spliceosome	5	0.0365
	Taste transduction	5	0.000835
	alpha-Linolenic acid metabolism	2	0.0328
	Dorso-ventral axis formation	2	0.0495

Table 2 Genes related to cell proliferation, oxidation, and muscle contraction

Gene symbol	Gene name	Fold	Direction	Description
Genes related to cell proliferation				
KLF6	Kruppel-like factor 6	5.66	↓	Functions as a tumor suppressor
SIRT6	Sirtuin 6	5.13	↓	Modulates acetylation of histone H3 in telomeric chromatin during the S-phase of the cell cycle
CASP10	Caspase 10	4.41	↓	Involved in activation cascade of caspases responsible for apoptosis execution
NLRP1	Pyrin domain containing 1	4.25	↓	Enhances APAF1 and cytochrome c-dependent activation of pro-caspase-9 and consecutive apoptosis.
TNFAIP1	Tumor necrosis factor, alpha-induced protein 1	3.17	↓	Interaction with RHOB may regulate apoptosis, regulating actin cytoskeleton and cell migration
C1QTNF1	C1q and tumor necrosis factor related protein 1	3.26	↓	Function as a apoptosis factors
MAPK15	mitogen-activated protein kinase 15	2.04	↑	In vitro, phosphorylates MBP
RHOB	Rho-related GTP-binding protein	2.03	↓	Mediates apoptosis in neoplastically transformed cells after DNA damage.
Genes related to actin cytoskeleton				
ACTR3B	actin-related protein 3 homolog B	5.27	↑	Regulatory role in actin cytoskeleton and induces cell-shape change and motility.
MPRIP	myosin phosphatase Rho interacting protein	5.20	↓	Targets myosin phosphatase to actin cytoskeleton. Required for regulation of actin cytoskeleton by RhoA and ROCK1.
TTN	titin	2.97	↑	Key component in assembly and functioning of vertebrate striated muscles
MYL7	myosin, light chain 7	2.89	↑	Muscle contraction
NMUR1	neuromedin U receptor 1	2.14	↓	Receptor for neuromedin-U and neuromedin-S neuropeptides
EDNRA	endothelin receptor type A	2.14	↓	Receptor for endothelin-1.
Genes related to oxidation				
AIG1	androgen-induced 1	7.68	↑	Plays a role in androgen-regulated growth of hair follicles
NOX4	NADPH oxidase 4	2.70	↑	Constitutive NADPH oxidase which generates superoxide intracellularly upon formation of a complex with CYBA/p22phox
MSRB2	Methionine-R-sulfoxide reductase B2	2.28	↓	Plays a role in preservation of mitochondrial integrity by decreasing intracellular reactive oxygen species build-up through its scavenging role
FMO1	methylaniline monooxygenase	2.25	↓	Involved in oxidative metabolism of a variety of xenobiotics such as drugs and pesticides.
DHRS11	dehydrogenase/reductase	2.13	↓	Can utilize both NADH and NADPH

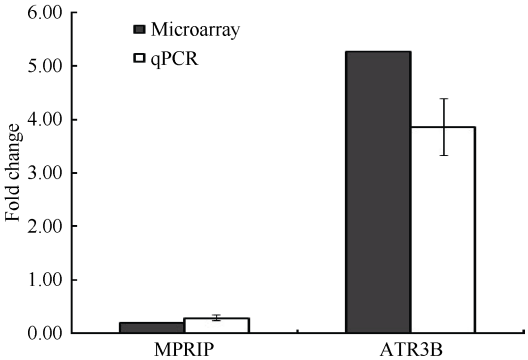

Figure 4 Comparisons between Q-polymerase chain reaction (qPCR) gene expression patter and microarray data between treated and control samples.

minimum 5-fold change in gene expression. Genes related to smooth muscle contraction such as ACTR3B and MPRIP were chosen based on their level of expression in the microarray study. As shown in Figure 4, the upregulated or downregulated patterns for ACTR3B and MPRIP obtained from qRT-PCR were similar to those in the microarray study.

CONCLUSION

The present work highlights the results of a series of in vitro studies, which demonstrated that oxidative stress and cytotoxicity were involved in the effect of Cr(VI) on HISM cells. In addition, here we provided a global view of differential gene expression in HISM cells in response to Cr(VI) induction and identified some novel changes in gene expression, such as MPRIP and TTN, that may be unique to smooth muscle cells in response to Cr(VI) induction. This study provides useful information not only for understanding molecular mechanisms in Cr(VI) toxicity, but also in advancing our knowledge in a number of fields.

References

Bucher J. 2007. NTP Toxicity Studies of Sodium Dichromate Dihydrate (CAS No. 7789-12-0) Administered in Drinking Water to Male and Female F344/N Rats and B6C3F1 Mice and Male BALB/c and am3-C57BL/6 Mice. *Toxicity Report Series,* (72): G1-G4.

Kimura T, Okumura F, Onodera A, Nakanishi T, Itoh N, Isobe M. 2011. Chromium (VI) inhibits mouse metallothionein-I gene transcription by modifying the transcription potential of the co-activator p300. *The Journal of Toxicological Sciences,* **36**(2): 173-180.

Koga Y, Ikebe M. 2005. p116Rip decreases myosin II phosphorylation by activating myosin light chain phosphatase and by inactivating RhoA. *The Journal of Biological Chemistry,* **280**(6): 4983-4991.

Kopec AK, Kim S, Forgacs AL, Zacharewski TR, Proctor DM, Harris MA, Haws LC, Thompson CM. 2012. Genome-wide gene expression effects in B6C3F1 mouse intestinal epithelia following 7 and 90days of exposure to hexavalent chromium in drinking water. *Toxicology and Applied Pharmacology,* **259**(1): 13-26.

Liu AH, He WS, Lin SY, Xiong XK, Zhao GF, Sun LH, Ji XM, Liu CL, Xuan XZ. 1991. Micronuclei of rat bone marrow cells and lung macrophages induced by five kinds of Yunnan Tin ore powder and four kinds of metallic compound. *Zoological Research,* **12**(3): 309-314. (in Chinese)

Myers JM, Antholine WE, Myers CR. 2011. The intracellular redox stress caused by hexavalent chromium is selective for proteins that have key roles in cell survival and thiol redox control. *Toxicology*, **281**(1-3): 37-47.

Park RM, Stayner LT. 2006. A search for thresholds and other nonlinearities in the relationship between hexavalent chromium and lung cancer. *Risk Analysis,* **26**(1): 79-88.

Rafael AI, Almeida A, Santos P, Parreira I, Madeira VM, Alves R, Cabrita AM, Alpoim MC. 2007. A role for transforming growth factor-beta apoptotic signaling pathway in liver injury induced by ingestion of water contaminated with high levels of Cr(VI). *Toxicology and Applied Pharmacology,* **224**(2): 163-173.

Raghunathan VK, Ellis EM, Grant MH. 2009. Response to chronic exposure to hexavalent chromium in human monocytes. *Toxicology in Vitro,* **23**(4): 647-652.

Shi D, Jiang BH. 2002. Antioxidant properties of apple juice and its protection against Cr(VI)-induced cellular injury. *Journal of Environmental Pathology Toxicology and Oncology,* **21**(3), 233-242.

Smith AH. 2008. Hexavalent chromium, yellow water, and cancer: a convoluted saga. *Epidemiology,* **19**(1): 24-26.

Stout MD, Herbert RA, Kissling GE, Collins BJ, Travlos GS, Witt KL, Melnick RL, Abdo KM, Malarkey DE, Hooth MJ. 2009. Hexavalent chromium is carcinogenic to F344/N rats and B6C3F1 mice after chronic oral exposure. *Environmental Health Perspectives,* **117**(5): 716-722.

Subramanian S, Rajendiran G, Sekhar P, Gowri C, Govindarajulu P, Aruldhas MM. 2006. Reproductive toxicity of chromium in adult bonnet monkeys (*Macaca radiata* Geoffrey). Reversible oxidative stress in the semen. *Toxicology and Applied Pharmacology,* **215**(3): 237-49.

Sun H, Clancy HA, Kluz T, Zavadil J, Costa M. 2011. Comparison of gene expression profiles in chromate transformed BEAS-2B cells. *PLoS One*, 6(3): e17982.

Surks HK, Riddick N, Ohtani K. 2005. M-RIP targets myosin phosphatase to stress fibers to regulate myosin light chain phosphorylation in vascular smooth muscle cells. *The Journal of Biological Chemistry,* **280**(52): 42543-4251.

Thompson CM, Proctor DM, Haws LC, Hebert CD, Grimes SD, Shertzer HG, Kopec AK, Hixon JG, Zacharewski TR, Harris MA. 2011. Investigation of the mode of action underlying the tumorigenic response induced in B6C3F1 mice exposed orally to hexavalent chromium. *Toxicological Sciences,* **123**(1): 58-70.

Velma V, Tchounwou PB. 2011. Hexavalent chromium-induced multiple biomarker responses in liver and kidney of goldfish, *Carassius auratus*. *Environmental Toxicology,* **26**(6): 649-656.

Ye J, Shi X. 2001. Gene expression profile in response to chromium-induced cell stress in A549 cells. *Molecular and Cellular Biochemistry,* **222**(1-2): 189-197.

Yuan Y, Ming Z, Gong HH, Lan G, Lu D, Peng L, Feng J, Zhong CG. 2012. Cr(VI) induces the decrease of ATP level and the increase of apoptosis rate mediated by ROS or VDAC1 in L-02 hepatocytes. *Environmental Toxicology and Pharmacology,* **34**(2): 579-587.

Zhang JD, Li SK. 1997. Cancer mortality in a Chinese population exposed to hexavalent chromium in water. *Journal of Occupational and Environmental Medicine,* **39**(4): 315-319.